
Inhibitory control of spike timing precision

Maxime Ambard and Dominique Martinez
CORTEX Group, LORIA-INRIA, Nancy, France
ambard@loria.fr, dmartine@loria.fr

Abstract

GABAergic inhibition via local interneurons may play a role in enhancing spike timing precision in principal cells, since it tends to eliminate the influence of initial conditions. However, both the number and the timing of inhibitory synaptic events may be variable across repeated trials. How does this variability affect the spike timing precision in principal neurons? In this paper, we derive an analytical expression for the spike output jitter as a function of the variability of the received inhibition. This study predicts that variable inhibition is especially tolerated as the number of inhibitory cells is large, which is consistent with experimental data from early olfactory systems (antennal lobe for insects, olfactory bulb for vertebrates).

1 Introduction

Experimental evidence tends to show that precise spike timing plays a significant role in the encoding of sensory stimuli [1]. A pre-requisite is that neurons fire spikes in a precise and reproducible way over repeated presentations of the same stimulus. Both experimental studies and theoretical works have shown that the neural response can indeed be precise and reliable, depending on the nature of the input [2, 3, 4]. Fast varying aperiodic stimuli lead to precise spike timing while constant or slowly varying stimuli yield imprecise firing. All natural stimuli however do not have a high-temporal bandwidth. For example, in comparison with sounds or images, odors change more slowly.

Olfaction is generally a slow-temporal bandwidth sense. Olfactory receptor neurons converge onto glomeruli that present a slow dynamics of activation [5]. Thus, olfactory bulb mitral cells (MCs), excited by one or few glomeruli, receive slowly varying inputs. It is known that MCs have an unreliable spiking activity under constant stimulation [6]. Despite this fact, some MCs present in vivo synchronisation with precise spiking activity [7, 8]. In the olfactory bulb, MCs receive inhibition from inhibitory granule cells (GCs). The received inhibition could be responsible of the precision of individual MCs, since it tends to eliminate the influence of initial conditions [9, 10]. However, GABA release from GCs is random [11], and thus inhibitory feedback into the MCs is a stochastic process. How does the stochastic nature of the received inhibition affect the precision of principal cells? To address this

question we shall use a quadratic integrate-and-fire neuron model that allows for analytic calculations. In section 2, we describe our model and present simulations showing that GABAergic inhibition may enhance spike timing precision. In section 3, we derive an approximate analytical expression for the spike output jitter as a function of the variability of the received inhibition. In section 4, we demonstrate the validity of this approximation with simulation results. In section 5, we discuss the predictions obtained from our study.

2 Model description and Simulations

We consider here the quadratic integrate and fire (QIF) model which is known to be a very good approximation of any type 1 neuron [12]. The time evolution of the membrane potential V is described by the following equation

$$C \frac{dV}{dt} = q(V(t) - V_T)^2 + I - I_{th} - I_{GABA}(t) + I_{noise}(t) \quad (1)$$

in which I is a constant input current, I_{th} denotes the minimal current required for repetitive firing, I_{noise} is an intrinsic white noise current of standard deviation σ_{noise} and I_{GABA} is a synaptic inhibitory current. In the absence of any noise and synaptic current, the QIF neuron converges to the resting potential V_{rest} when $I = 0$ and fires as soon as V reaches the threshold V_{th} , when $I \geq I_{th}$. Right after the spike, V is reset to the value V_{reset} . The membrane capacitance C and resting potential V_{rest} have been derived from MC experimental data [13] [14]. The other parameters have been fitted in order to obtain a similar frequency-current response than the MC conductance based model in [15]. The parameters chosen for the QIF neuron are as follows : $C = 0.2$ nF, $V_{rest} = -65$ mV, $V_T = -60.68$ mV, $q = 0.00643$ mS.V⁻¹, $I_{th} = 0.12$ nA, $V_{th} = 30$ mV and $V_{reset} = -70$ mv.

The inhibitory synaptic current $I_{GABA}(t)$ in Eq. 1 results from the summation of GABAergic synaptic events originating from interactions with GCs. An unitary event, occurring at time t^f , is modeled by a simple exponential inhibitory post-synaptic current (IPSC). For $t \geq t^f$, we have

$$IPSC(t) = g e^{-(t-t^f)/\tau} (V(t) - E_{GABA}) \quad (2)$$

The maximum synaptic conductance is $g = 1$ nS [14], the synaptic time decay is $\tau = 6$ ms [16] and the reversal potential of the synapse is $E_{GABA} = -70$ mV.

The QIF neuron is precise when its firing time T stays unchanged across repeated trials with the same input current I . A measure of precision is the spike time jitter σ_T which characterizes the temporal dispersion around cluster firing times induced by repeated trials (precise neuron = small σ_T). Figure 1 shows the temporal evolution of σ_T , estimated over 100 repeated simulations of the QIF neuron (Eq. 1), with $I_{GABA} = 0$ and different σ_{noise} values. The initial condition $V(t = 0)$ was similar in all trials. Due to I_{noise} , the spike time jitter σ_T increases over time so that the neuron becomes more and more imprecise. This is in agreement with previous works [2, 3, 4]. To see if the first spike can convey some information about the input, we performed repeated simulations for different I and random initial conditions. Figure 2 shows the mean and standard deviation σ_T of the first spike latency for a QIF neuron, with and without GABAergic inhibition. When $I_{GABA} \neq 0$, 100 synchronous IPSCs are generated at time $t^f = 0$ according to Eq. 2. From Fig. 2, we see that σ_T is very large when $I_{GABA} = 0$ and very small when $I_{GABA} \neq 0$. GABAergic inhibition makes the neuron more precise so that its firing

time T is a reliable estimate of I . Two examples of spike rasters are indicated in Fig. 2 for $I = 0.14nA$ and for $I_{GABA} = 0$ and $I_{GABA} \neq 0$.

In our simulations, GABAergic inhibition tends to eliminate the influence of initial conditions, in line with previous works [9, 10]. In the olfactory bulb, the received inhibition from GCs could therefore be responsible for the precision of individual MCs. However, GABA release from GCs is random [11] and thus inhibitory feedback into the MCs will be variable across trials. How does the variability of the received inhibition affect the precision of principal neurons? This point will be studied mathematically in the next section.

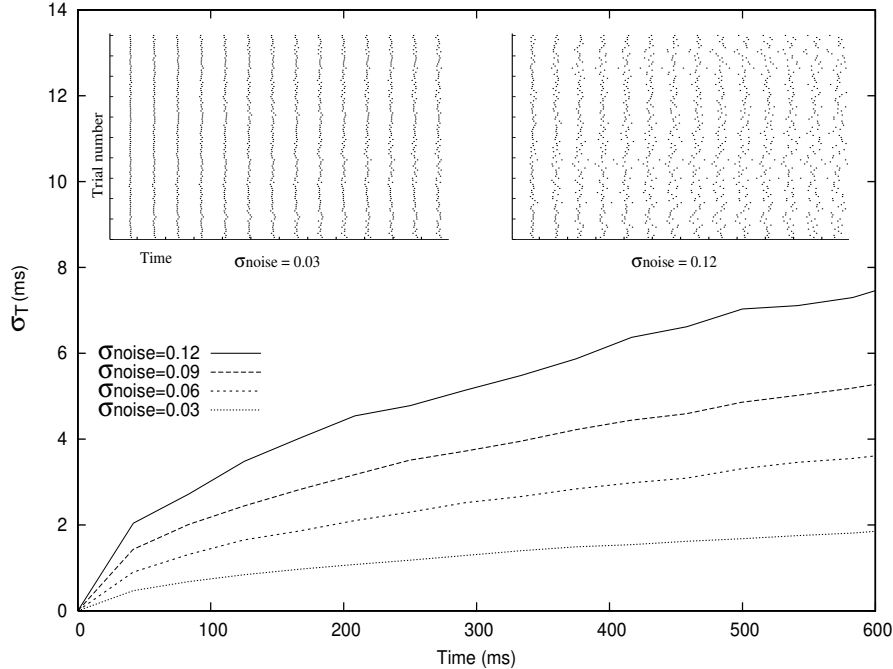


Figure 1: **Without GABAergic inhibition, the spike time jitter σ_T increases over time.** The different curves indicate the temporal evolution of the spike time jitter σ_T estimated over 100 repeated simulations of the QIF neuron (Eq. 1). In the simulations, $I = 0.15nA$, $I_{GABA} = 0$ and σ_{noise} ranges from 0.03 to 0.12nA. Two examples of spike rasters obtained from 100 trials are indicated for $\sigma_{noise} = 0.03$ and 0.12nA.

3 Mathematical analysis of spike timing precision for a neuron receiving variable inhibition

Let us first consider a QIF neuron (Eq. 1 with $I_{noise}(t) = 0$) receiving, at a time t^f , a single IPSC whose temporal evolution is given by Eq. 2. The total current, for $t \geq t^f$, is then

$$J(t) = I - I_{th} - ge^{-(t-t^f)/\tau}(V(t) - E_{GABA}) \quad (3)$$

Börger and Kopell [9] have shown that the firing time T_1 of a QIF neuron receiving a single strong IPSC is relatively independent of the initial condition $V(t = 0)$, see

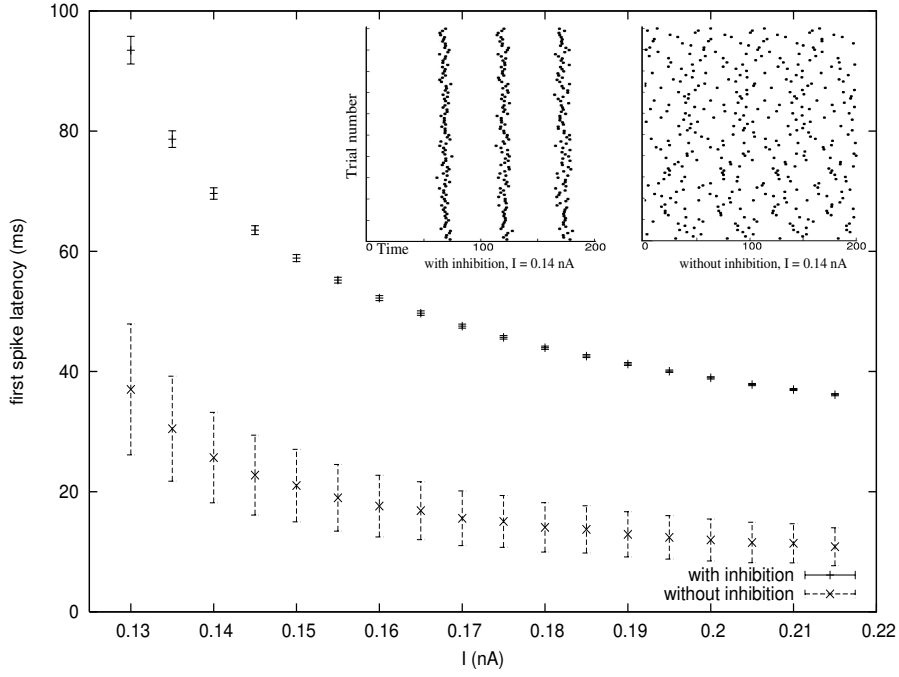


Figure 2: **Synchronous GABAergic inhibition enhances spike timing precision.** Mean and standard deviation of the first spike latency as a function of the input current I have been estimated over 100 repeated simulations of the QIF neuron (Eq. 1, $\sigma_{noise} = 0.05 nA$). The top curve is for $I_{GABA} \neq 0$ whereas the one at the bottom is for $I_{GABA} = 0$. $I_{GABA} \neq 0$ was obtained by the summation of 100 synchronous synaptic events occurring at time $t^f = 0$ and modeled by Eq. 2. Two spike rasters, obtained from repeated trials with $I = 0.14 nA$, are indicated for $I_{GABA} = 0$ and $I_{GABA} \neq 0$.

also [10]. Provided g is large enough, trajectories in the phase plane (V, J) are all attracted towards a given trajectory so that they all reach approximately the same point (V_{th}, J^*) at firing time. This is shown in Fig. 3 in [9] and Fig. 5C in [10]. The result is an almost complete loss of the initial condition $V(t = 0)$. Whatever the initial condition might be, the total input current is approximately equal to J^* at the firing time T_1

$$J^* \approx J(T_1) = I - I_{th} - g e^{-(T_1 - t^f)/\tau} (V_{th} - E_{GABA})$$

and thus

$$T_1 \approx \tau \ln g - \tau \ln(I - I_{th} - J^*) + \tau \ln(V_{th} - E_{GABA}) + t^f$$

To determine the effect of variable inhibition on the spike time jitter, we have generalized Börgers and Kopell's study to the case of a QIF neuron receiving a burst of k IPSCs at times t_i^f , $i = 1, 2 \dots k$. Without loss of generality, we consider that the neuron fires after receiving the k th IPSC. At the firing time T , the total

input current is approximately equal to J^*

$$J^* \approx J(T) = I - I_{th} - \sum_{i=1}^k g e^{-(T-t_i^f)/\tau} (V_{th} - E_{GABA})$$

and thus, the firing time of a neuron receiving a burst of k IPSCs is

$$T \approx \tau \ln g - \tau \ln(I - I_{th} - J^*) + \tau \ln(V_{th} - E_{GABA}) + \tau \ln \sum_{i=1}^k e^{t_i^f/\tau} \quad (4)$$

Let us now consider variable inhibition, i.e. the number k of received IPSCs is a random variable with mean $\langle k \rangle$ and variance σ_k^2 , and the IPSC times t_i^f are drawn randomly from an unknown probability density function with variance σ_t^2 . The only random variable in Eq. (4) is thus

$$X = \tau \ln \sum_{i=1}^k e^{t_i^f/\tau}$$

Furthermore, we have $\sigma_T^2 = \sigma_X^2$. An approximation for σ_T^2 can be found by considering the fact that the variance of a sum of a random number k of independent random variables, each with variance σ^2 , is $\langle k \rangle \sigma^2 + \langle k \rangle^2 \sigma_k^2$, and that the variance of a function $y = g(x)$ of a random variable x approximately depends on the mean η_x and variance σ_x^2 of x : $\sigma_y^2 \approx |dg/dx|_{x=\eta}^2 \sigma_x^2$ (eq. 5-56 in [17]). Using these formulae, we found

$$\sigma_T^2 \approx \frac{1}{\langle k \rangle} \left(\sigma_t^2 + \tau^2 \frac{\sigma_k^2}{\langle k \rangle} \right) \quad (5)$$

Note that Eq. 5 becomes identical to Eq. (4.20) in [9] when the inhibition is precise ($\sigma_t^2 = 0$). However, Eq. 5 is more general than the one in [9] because it takes into account the fact that the IPSCs can occur at different times.

4 Numerical results

In order to check the validity of the approximation given by Eq. 5, we performed repeated simulations of the QIF neuron (Eq. 1, $I_{noise}(t) = 0$) receiving a burst of k stochastic asynchronous synaptic events (Eq. 2). The number k of unitary IPSCs is drawn randomly from a gaussian density with mean $\langle k \rangle = 100$ and standard deviation σ_k varying from 0 to 9. Unitary IPSCs are generated at random times (inhibitory jitter σ_t taken from 0 to 9 ms). Figure 3 compares the theoretical spike time jitter σ_T given by Eq. 5 to the one obtained from simulations. When the inhibition is precise (small σ_t) and balanced ($k \approx \langle k \rangle$, small σ_k), we see a perfect match between theoretical and experimental σ_T values. For σ_t larger than 4 ms, σ_T values given by Eq. 5 are however underestimated. Moreover, the discrepancy between theoretical and experimental σ_T values increases with the inhibitory jitter σ_t . This is due to the approximations made for deriving Eq. 5. In particular, the approximation of the variance of a function (eq. 5-56 in [17]) is only valid when the variance is small. From Eq. 5, we see that the inhibitory jitter contributes negatively to the spike timing precision through the ratio $\sigma_t^2 / \langle k \rangle$. Because the mean number

of IPSCs was large in our simulations, we obtained $\sigma_T \ll \sigma_t$ (see Fig. 3). So far, we just considered a single burst of inhibition with $\langle k \rangle$ fairly large. What happens to the spike time jitter when $\langle k \rangle$ is smaller and the inhibition phasic? To address this question, we performed simulations of a QIF neuron receiving consecutive bursts of stochastic asynchronous synaptic events. Figure 4 shows the temporal evolution of σ_T after consecutive bursts of inhibition. We see that σ_T reaches a stable state that does not depend on initial conditions but does depend on the value of σ_k .

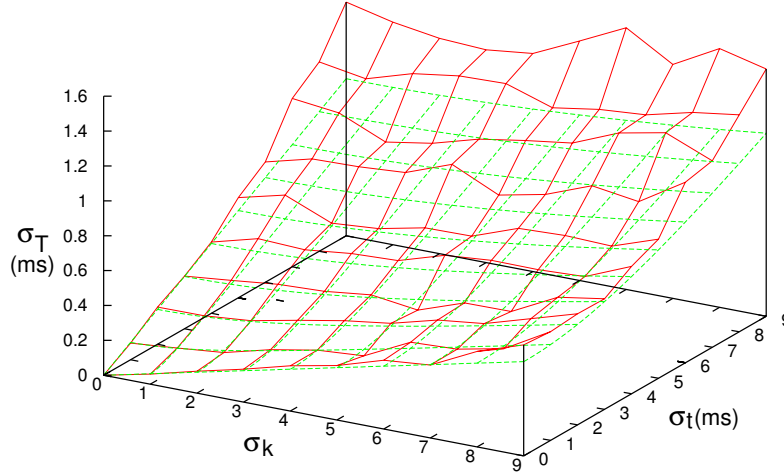


Figure 3: **Spike time jitter σ_T as a function of the variability of the received inhibition (σ_t, σ_k).** The dashed curve represents theoretical σ_T values given by Eq. 5. The plain curve represents experimental σ_T values obtained from simulations of the QIF neuron. In Eq. 1, $I_{noise}(t) = 0$, $I = 0.13nA$ and I_{GABA} was obtained from a burst of k stochastic asynchronous synaptic events (Eq. 2). The number k of unitary IPSCs is drawn randomly from a gaussian density with mean $\langle k \rangle = 100$ and standard deviation σ_k varying from 0 to 9. Unitary IPSCs are generated at random times (inhibitory jitter σ_t taken from 0 to 9 ms).

5 Discussion

We have considered the spike timing precision of a neuron receiving GABAergic inhibition. Due to the stochastic nature of the inhibition, the number and the timing of inhibitory synaptic events is variable across repeated trials. How does this variability affect the spike timing precision in principal neurons? We have derived an approximate analytical expression for the spike output jitter (Eq. 5). The variability of the received inhibition is characterized by the inhibitory jitter σ_t^2 and the variance σ_k^2 in the number k of inhibitory events. The inhibition is said to be balanced when σ_k^2 is small so that k across trials is approximately equal to the mean inhibition $\langle k \rangle$. The inhibition is said to be precise when σ_t^2 is small so that the inhibitory events occur approximately at the same time. From Eq. 5, we see

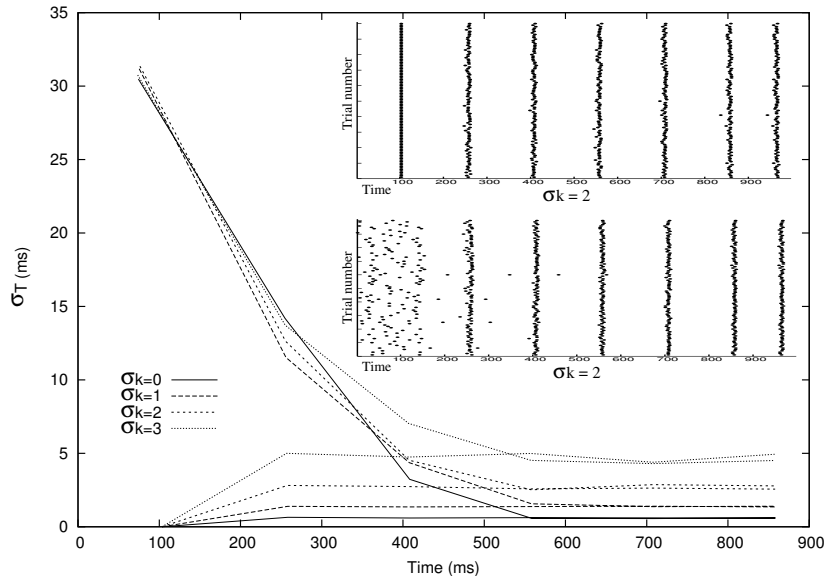


Figure 4: **With phasic GABAergic inhibition, the temporal evolution of the spike time jitter σ_T reaches a stable state.** The QIF neuron (Eq. 1, $I_{noise}(t) = 0$) receives consecutive bursts of stochastic asynchronous synaptic events ($\langle k \rangle = 10$ IPSCs, $\sigma_t = 2$ ms, σ_k varying from 0 to 3 IPSCs, period of inhibitory bursts = 150 ms). Two extreme initial conditions are considered, one for which $V(t = 0)$ was similar in all trials and another for which $V(t = 0)$ was randomly chosen. They respectively lead to $\sigma_T = 0$ ms and $\sigma_T \approx 30$ ms at time $t = 100$ ms. Despite different initial conditions, σ_T converges to a stable state which depends on the value of σ_k . Two spike rasters, obtained from repeated trials with $I = 0.125nA$, are indicated for the two initial conditions.

that the contribution of σ_t^2 and σ_k^2 to the spike output jitter σ_T^2 is divided by the mean inhibition $\langle k \rangle$ (large $\langle k \rangle$ implies small σ_T^2).

In neural structures with a large number of inhibitory cells, $\langle k \rangle$ is expected to be large, and thus there is no requirement to have precise and balanced inhibition. In contrast, precise spike timing in neural structures where $\langle k \rangle$ is small requires precise and balanced inhibition. This prediction is in line with previous work [18]. It is also in agreement with experimental data from early olfactory systems (antennal lobe for insects, olfactory bulb for vertebrates). On the one hand, the olfactory bulb has a large number of inhibitory cells (e.g. $\sim 10^6$ for the mouse) and the inhibition is not precise ($\sigma_t \approx 22$ ms, see Fig. 4B2 in [16]). On the other hand, the antennal lobe has a small number of inhibitory cells (e.g. 300 for the locust) and the inhibition is very precise ($\sigma_t \approx 3.8$ ms, see [19]).

Other lines of research as extensions to this work are interesting to pursue, in particular the role of phasic inhibition. As seen in Fig. 4, the firing times of a neuron receiving consecutive bursts of inhibition become more and more precise over time. On the contrary, the spike time jitter of a residual neuron that does not receive inhibition increases over time so that only its firing rate can reliably encode information (see Fig. 1). This suggests that complementary pieces of information may be conveyed in the precise timing of inhibited neurons and in the firing rate

of residual neurons. Phasic inhibition could therefore multiplex information into separate channels, in agreement with recent experimental work [8].

References

- [1] R. VanRullen, R. Guyonneau, and S. J. Thorpe. Spike times make sense. *Trends in Neurosciences*, 28:1–4, 2005.
- [2] Z. Mainen and T. Sejnowski. Reliability of spike timing in neocortical neurons. *Science*, 268:1503–1506, 1995.
- [3] R. Brette and E. Guigon. Reliability of spike timing is a general property of spiking model neurons. *Neural Computation*, 15:279–308, 2002.
- [4] B. Gutkin, G. B. Ermentrout, and M. Rudolph. Spike generating dynamics and the conditions for spike-time precision in cortical neurons. *J. Comput. Neuroscience*, 15:91–103, 2003.
- [5] S. Sachse and C. G. Galizia. The coding of odour-intensity in the honeybee antennal lobe: local computation optimizes odour representation. *Eur. J. Neurosci.*, 18:2119–2132, 2003.
- [6] R. Balu, P. Larimer, and B. W. Strowbridge. Phasic stimuli evoke precisely timed in intermittently discharging mitral cells. *J. Neurophysiol*, 92:743–753, august 2004.
- [7] H. Kashiwadani, Y. F. Sasaki, N. Uchida, and K. Mori. Synchronized oscillatory discharges of mitral/tufted cells with different molecular receptive ranges in the rabbit olfactory bulb. *Journal of Neurophysiology*, 82:1786–1792, 1999.
- [8] R. W. Friedrich, C. J. Habermann, and G. Laurent. Multiplexing using synchrony in the zebrafish olfactory bulb. *Nature Neuroscience*, 7:862–871, 2004.
- [9] C. Börgers and N. Kopell. Synchronisation in network of excitatory and inhibitory neurons with sparse, random connectivity. *Neural Computation*, 15:509–538, 2003.
- [10] N. Kopell and B. Ermentrout. Chemical and electrical synapses perform complementary roles in synchronization of interneuronal networks. *PNAS*, 101:15482–15487, 2004.
- [11] V. Egger, K. Svoboda, and Z. F. Mainen. Dendrodendritic synaptic signals in olfactory bulb granule cells: local spine boost and global low-threshold spike. *The journal of neuroscience*, 25:3521–3530, 2005.
- [12] B. Ermentrout. Type 1 membranes, phase resetting curves, and synchrony. *Neural computation*, 8:979–1001, 1996.
- [13] G. Lowe. Inhibition of backpropagating action potential in mitral cell secondary dendrites. *J. Neurophysiol.*, 88:64–85, 2002.
- [14] Z. Nusser. Release-independent short-term facilitation on gabaergic synapses in the olfactory bulb. *Neuropharmacology*, 43:573–583, 2002.
- [15] G. Y. Shen, W. R. Chen, J. Mitdgaard, G. M. Shepherd, and M. L. Hines. Computational analysis of action potential initiation in mitral cell soma and dendrites based on dual patch recordings. *J. Neurophysiol.*, 82:3006–3020, 1999.
- [16] T. W. Margrie and A. T. Schaefer. Theta oscillation coupled spike latencies yield computational vigour in a mammalian sensory system. *J. Physiol*, 2002.
- [17] A. Papoulis. *Probability, random variables, and stochastic processes, second edition*. McGraw-Hill Book Co., New York, 1984.
- [18] D. Martinez. Oscillatory synchronization requires precise and balanced feedback inhibition in a model of the insect antennal lobe. *Neural Computation*, *In press*, 2005.
- [19] G. Laurent and H. Davidowitz. Encoding of olfactory information with oscillating neural assemblies. *Science*, 265:1872–1875, 1994.